Electronic Supplementary Material (ESI) for Dalton Transactions.

Electronic Supplementary Information

Simultaneous hetero-atom doping and foreign-thiolate exchanging on the $Au_{25}(SR)_{18}$ nanocluster

Xiao Wei,[a] Xi Kang,[a] Shuxin Wang,*[,a] Manzhou Zhu*[,a]

Experimental Details

1. Chemicals: Tetrachloroauric(III) acid ($HAuCl_4 \cdot 3H_2O$, > 99.99% gold basis), 4-mercaptobenzoic acid ($C_7H_6O_2S$, > 90%), silver nitrate ($AgNO_3$, 99.85%, metal basis), 2-phenylethanethiol (PhC_2H_4SH, > 98%), 4-bromothiophenol (BrC_6H_4SH, > 97%), 4-Aminothiophenol (C_6H_7NS, > 98%), sodium borohydride ($NaBH_4$, > 98%), tetraoctylammonium bromide (TOAB, 98%), ethanethiol (C_2H_5SH, 98%) were gained from ACROS Organic. Methanol (HPLC grade, ≥ 99.9%), tetrahydrofuran (HPLC grade, ≥ 99.9%), acetonitrile (HPLC grade, ≥ 99.9%) and methylene chloride (HPLC grade, ≥ 99.9%) were gained from Sigma-Aldrich. Pure water was purchased from Wahaha Co., LTD.

2. Synthesis of $Au_{25}(SC_2H_4Ph)_{18}^-$ TOA^+ nanoclusters

$HAuCl_4 \cdot 3H_2O$ (0.2 g/mL, 0.8 mL) and TOAB (0.254 g, 0.47 mmol) was dissolved in 14 mL of tetrahydrofuran in a 50 mL tri-neck round bottom flask. After ~15 min stirring (1500 rpm), phase transfer was completed and the color of the solution changed from yellow to red. Then, $PhCH_2CH_2SH$ (0.28 mL, 3 equivalents per the moles of the gold) was added to the solution under a stirring speed of ~1500 rpm. After the solution turned to clear (20 minutes), an aqueous solution of $NaBH_4$ (0.1550 g, 4 mmol) with ice water (5 mL) was quickly added to the above solution. The reaction was allowed to proceed about 5 hours. After that, the aqueous layer (at the bottom of the flask) was removed, and the tetrahydrofuran solution was centrifuged. Then the solution layer was raised and dried by rotavaporation. Methanol (20 mL) was added to remove the by-products and such wash/centrifugation cycle was repeated for 3 times. Then 10 mL of acetonitrile was used to extract pure $Au_{25}(SC_2H_4Ph)^-TOA^+$ nanocluster.

3. Synthesis of Ag-SC_2H_5 complexes

30 mg of silver nitrate was added in 7 mL of centrifuge tube which contained 2 mL of methanol. The ultrasonic dissolving method was used to dissolve the $AgNO_3$. Then, C_2H_5SH was added to the above solution and reacted for 5 minutes. The white solution was centrifuged and the solution layer was removed. Methanol (5 mL) was added in to remove needless ethanethiol and such wash/centrifugation cycle was repeated for 3 times.

4. Synthesis of Ag-SC_6H_4Br, AgS-C_6H_4COOH, AgS-$C_6H_4NH_2$ complexes

This synthesis method is similar to the Ag-SC_2H_5.

5. Details of the reaction tracking with UV-Vis and matrix-assisted laser desorption ionization-time of flight mass spectrometry (MALDI-MS for short)

UV-Vis absorption spectra were obtained using an Agilent 8453 instrument, and solution samples were prepared using CH_2Cl_2 as the solvent. MALDI-MS was recorded on a Bruker Autoflex III smart beam instrument, using trans-2-[3-(4-tert-butylphenyl)-2-methyl-2-propenylidene] malononitrile (DCTB) as a matrix. 5 mg of $Au_{25}(SC_2H_4Ph)_{18}^-$ TOA^+ was added in a 50 mL tri-neck round bottom flask and dissolved in 20 mL of CH_2Cl_2. Then 5 mg of Ag-SR was dissolved by 5 mL of CH_2Cl_2 and straw dropped to the above solution. The UV-vis and MALDI-MS of the reaction were monitored until the absorptions of the products became steady.

6. The purity of the as-prepared Au clusters was analyzed by size exclusion chromatography (SEC) on an Agilent 1200 Infinity Series using a PLgel column (particle size: 3 μm, pore diameter: 100 Å). A diode array detector (DAD) in situ monitors the optical absorption spectrum (210-850 nm range) of the eluted solution. The purity of the clusters can be verified by comparing the UV-vis spectra at different times of the peak (e.g. peak point, and left and right points at half height).

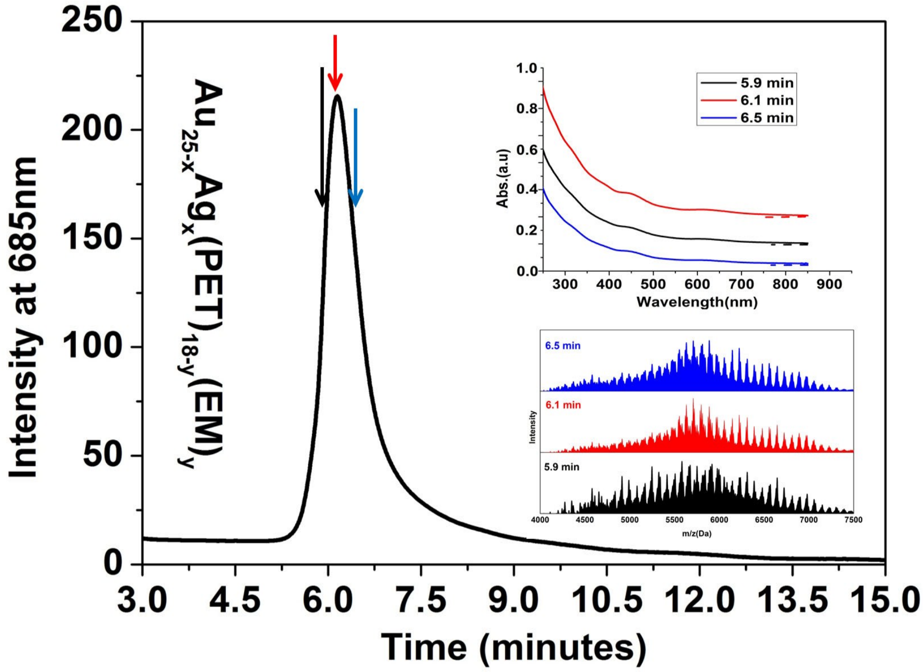

Fig. S1 HPLC results of the product of the M_{25} alloy nanoclusters. Insets: UV-vis spectra and ESI-MS results of the product in the three points.

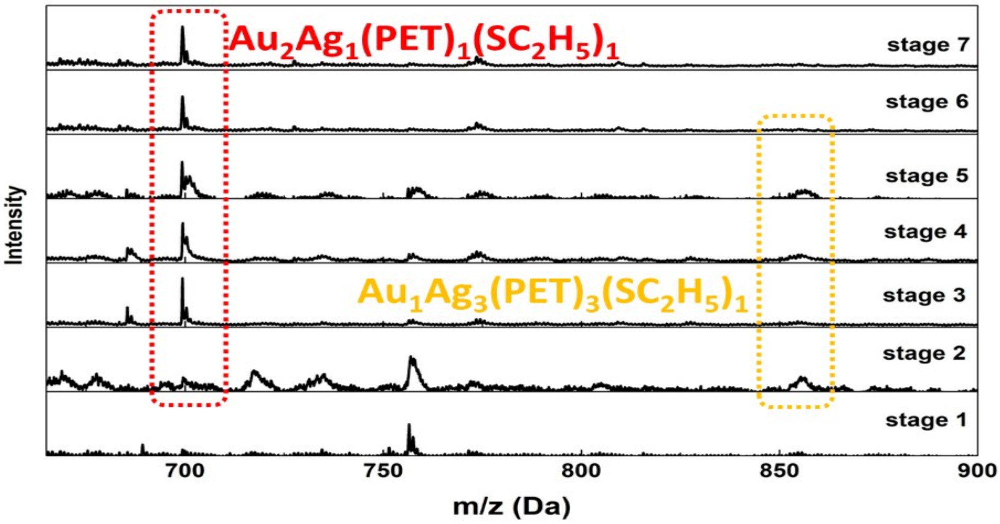

Fig. S2 Time-dependent MALDI-MS spectra (in the 650-900 Da range) of the metal/ligand-exchange process of doping $Au_{25}(PET)_{18}$ with Ag-SC_2H_5 complexes. X-axis represents the mass range and the Y-axis represents the intensity of the peaks.

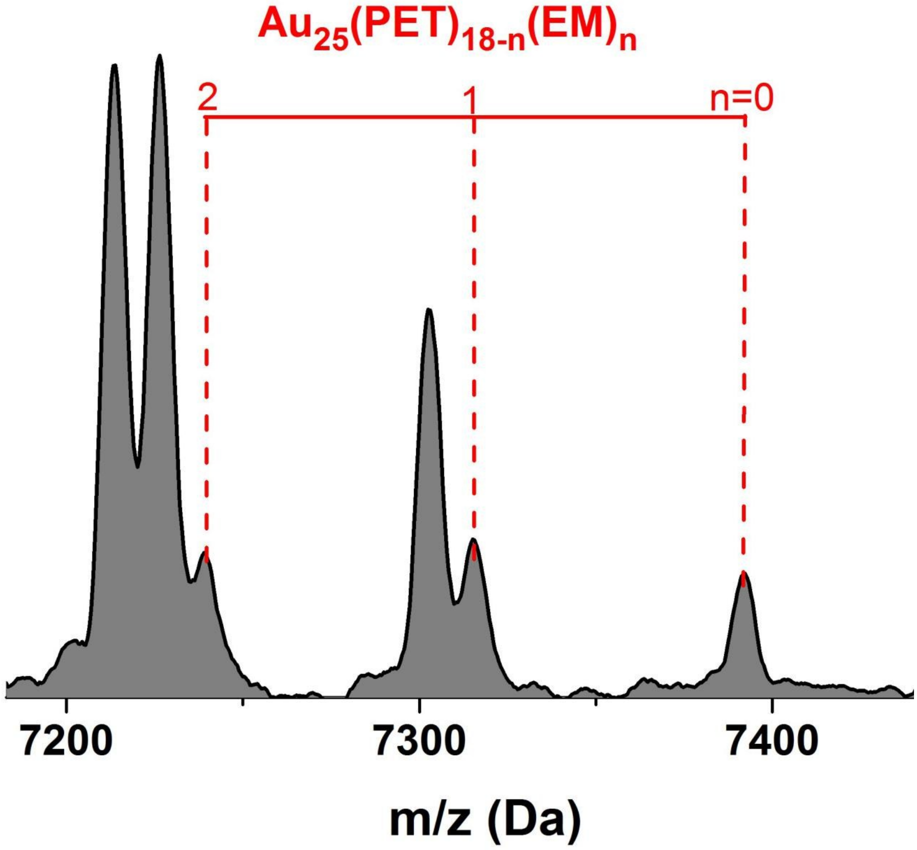

Fig. S3 MALDI-MS spectra of $Au_{25}(PET)_{18-n}(SC_2H_5)_n$ corresponding to stage 5 (where, n represents the number of S-C_2H_5, EM for short). The specific m/z and intensity of $Au_{25}(PET)_{18-n}(SC_2H_5)_n$ can be found in Tables S1 and S2, respectively.

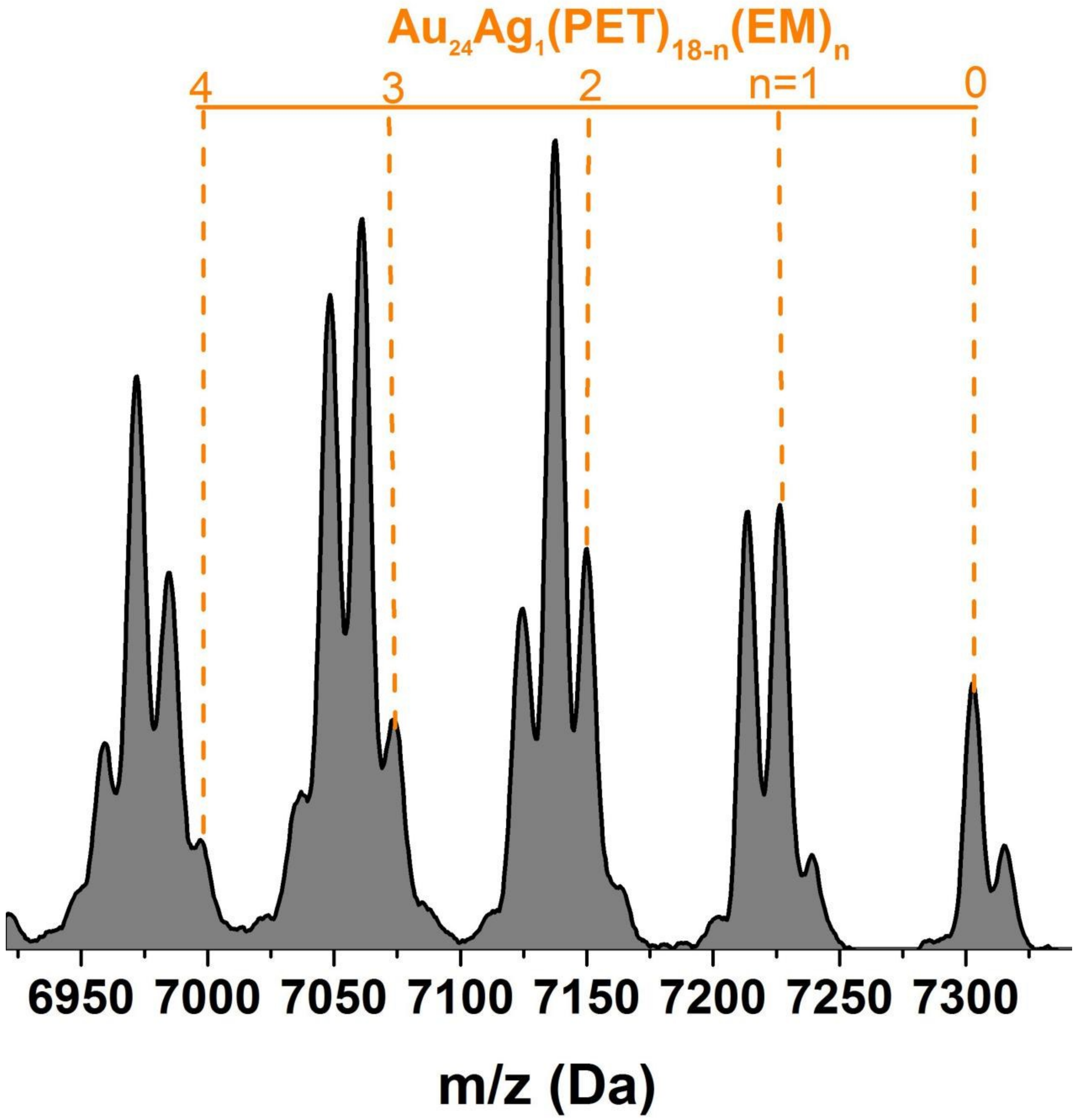

Fig. S4 MALDI-MS spectra of $Au_{24}Ag_1(PET)_{18-n}(SC_2H_5)_n$ corresponding to stage 5. The specific m/z and intensity of $Au_{24}Ag_1(PET)_{18-n}(SC_2H_5)_n$ can be found in Tables S1 and S2, respectively.

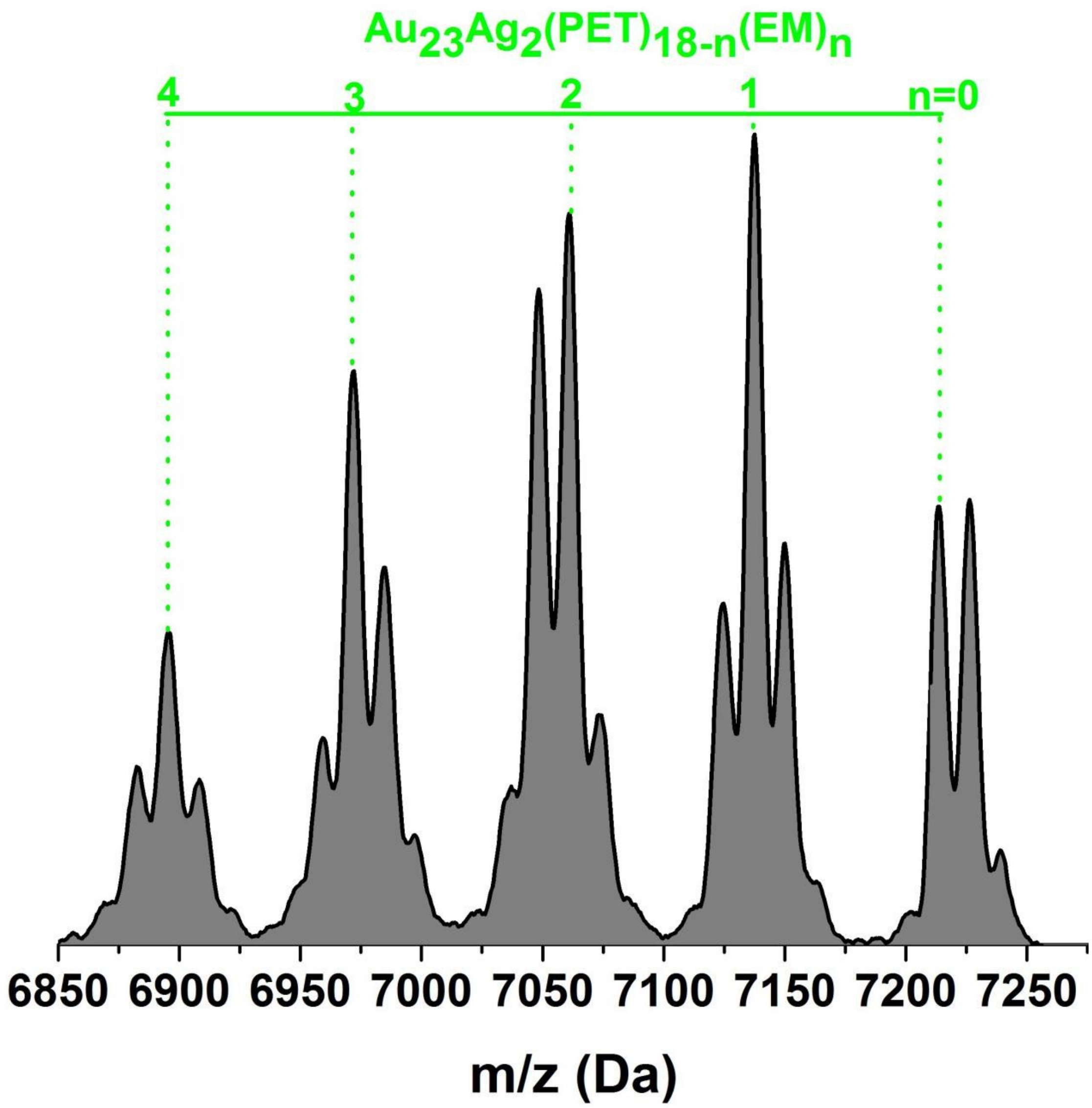

Fig. S5 MALDI-MS spectra of $Au_{23}Ag_2(PET)_{18-n}(SC_2H_5)_n$ corresponding to stage 5. The specific m/z and intensity of $Au_{23}Ag_2(PET)_{18-n}(SC_2H_5)_n$ can be found in Tables S1 and S2, respectively.

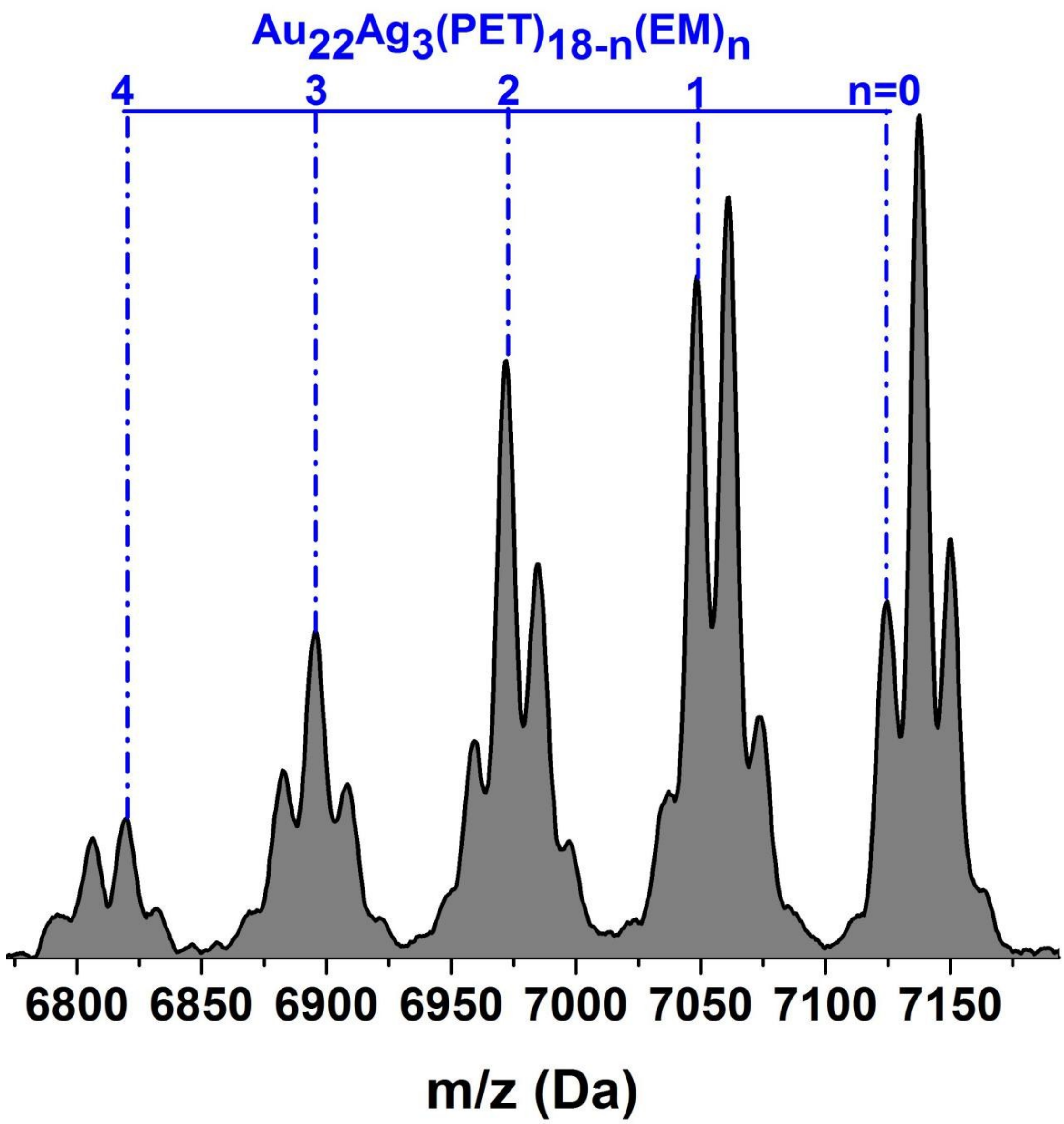

Fig. S6 MALDI-MS spectra of $Au_{22}Ag_3(PET)_{18-n}(SC_2H_5)_n$ corresponding to stage 5. The specific m/z and intensity of $Au_{22}Ag_3(PET)_{18-n}(SC_2H_5)_n$ can be found in Tables S1 and S2, respectively.

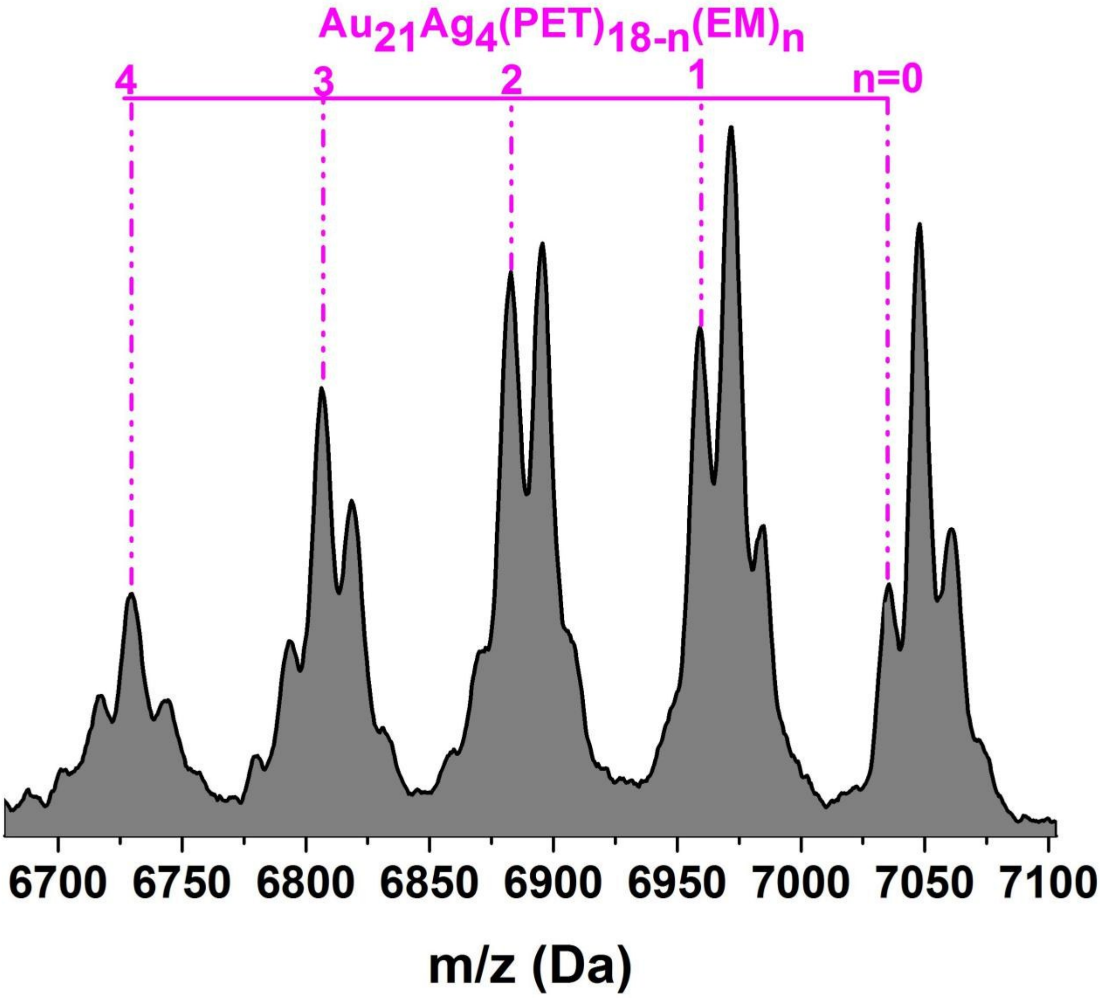

Fig. S7 MALDI-MS spectra of $Au_{21}Ag_4(PET)_{18-n}(SC_2H_5)_n$ corresponding to stage 6. The specific m/z and intensity of $Au_{21}Ag_4(PET)_{18-n}(SC_2H_5)_n$ can be found in Tables S1 and S2, respectively.

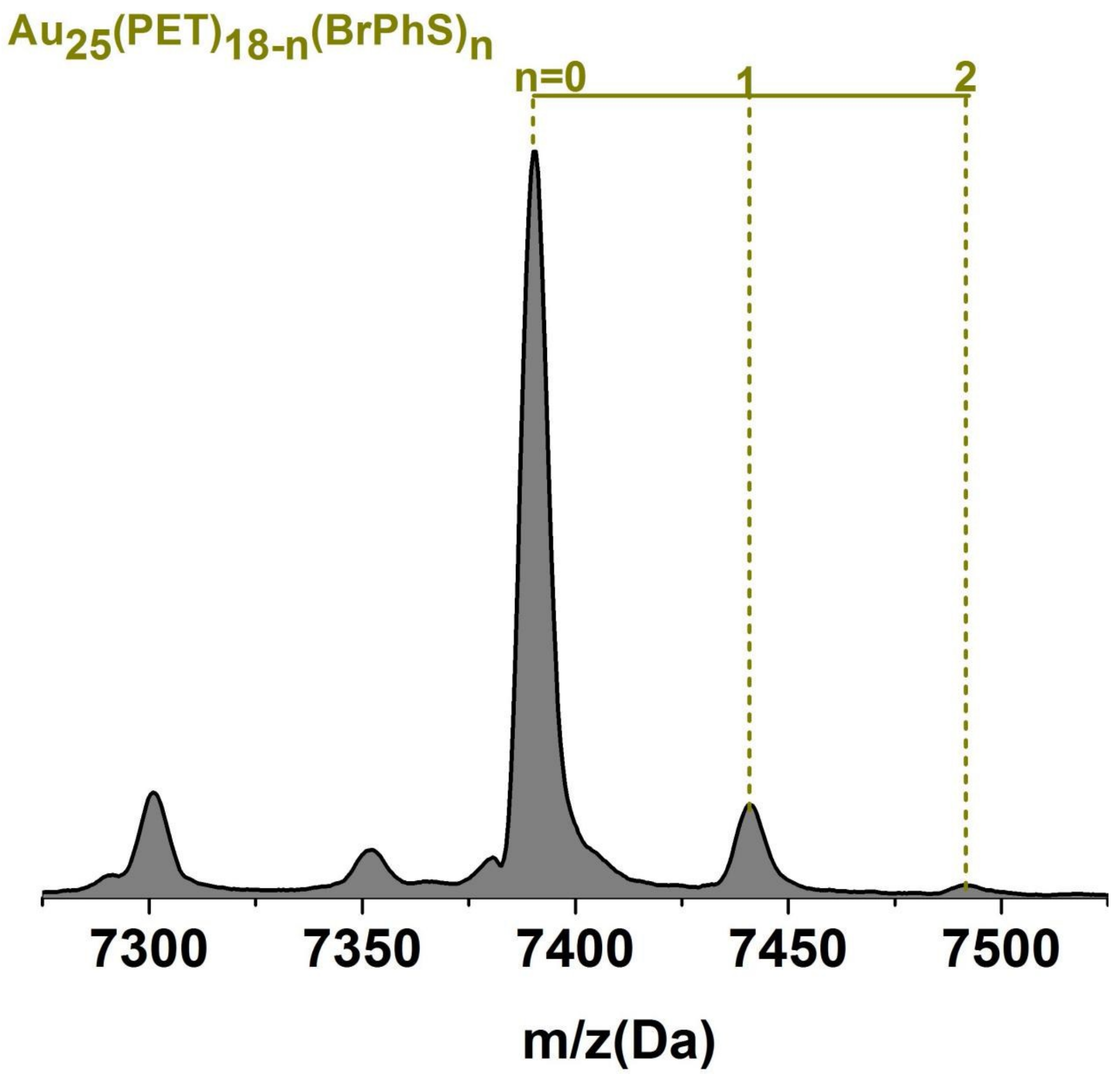

Fig. S8 MALDI-MS spectra of $Au_{25}(PET)_{18-n}(SPhBr)_n$ corresponding to stage 2 (where n represents the number of S-PhBr). The specific m/z and intensity of $Au_{25}(PET)_{18-n}(SPhBr)_n$ can be found in Tables S3 and S4, respectively.

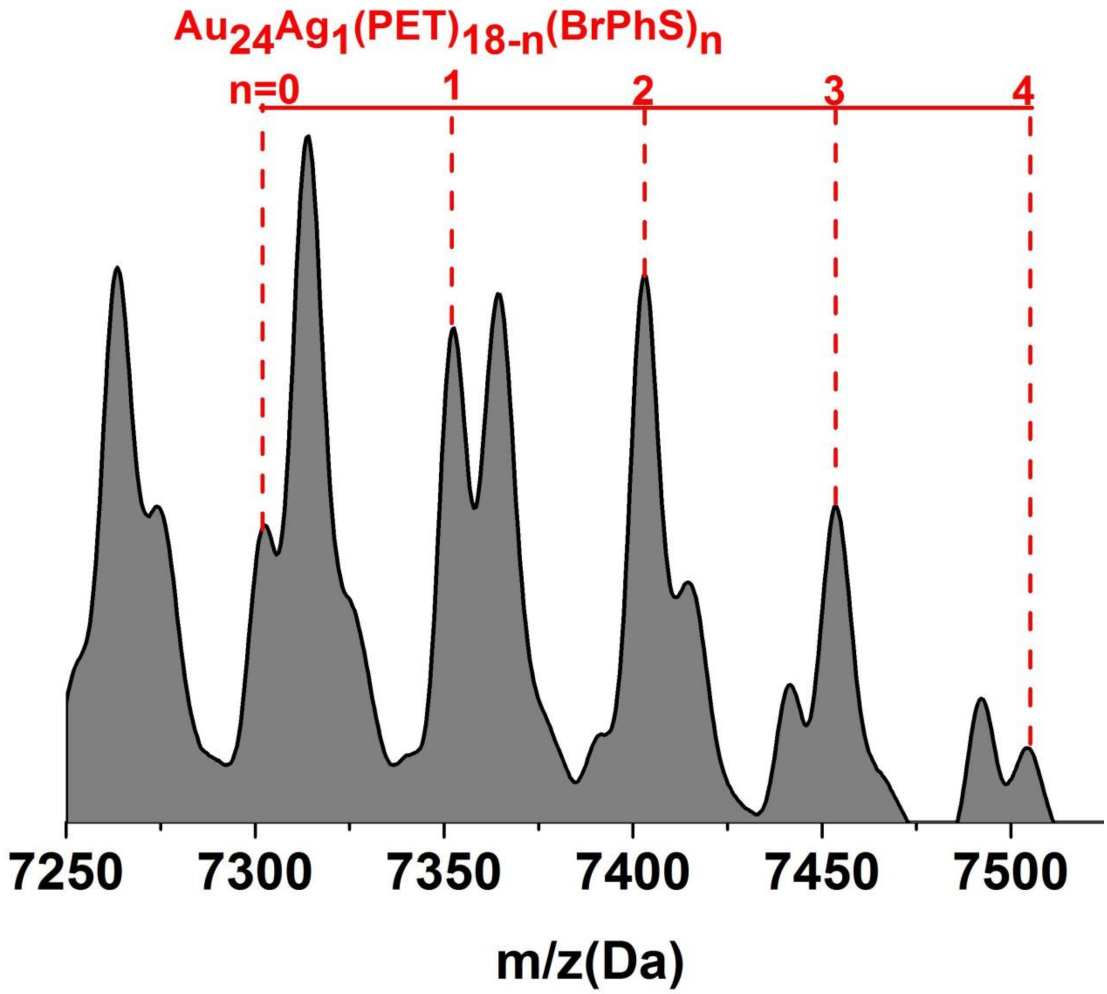

Fig. S9 MALDI-MS spectra of $Au_{24}Ag_1(PET)_{18-n}(SPhBr)_n$ corresponding to stage 7. The specific m/z and intensity of $Au_{24}Ag_1(PET)_{18-n}(SPhBr)_n$ can be found in Tables S3 and S4, respectively.

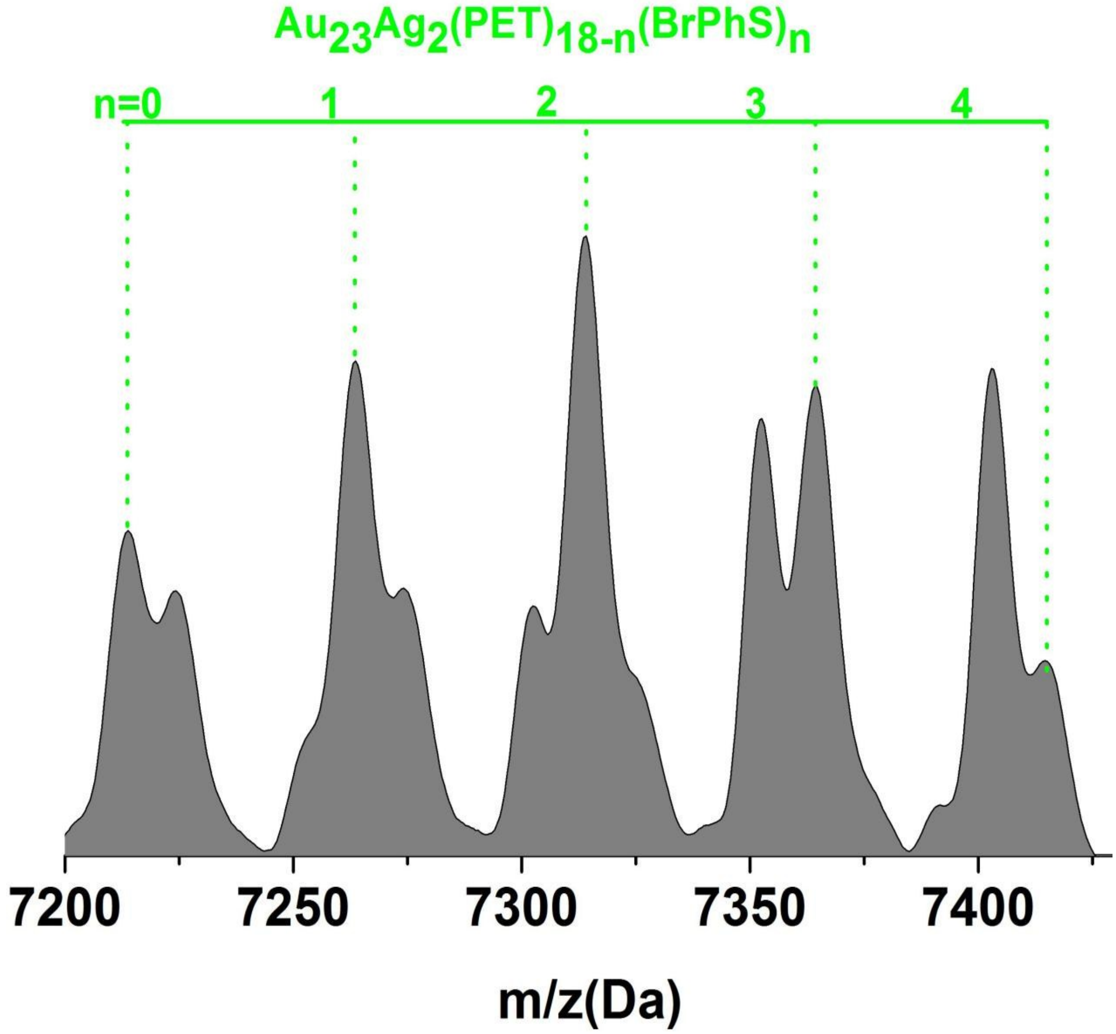

Fig. S10 MALDI-MS spectra of $Au_{23}Ag_2(PET)_{18-n}(SPhBr)_n$ corresponding to stage 7. The specific m/z and intensity of $Au_{23}Ag_2(PET)_{18-n}(SPhBr)_n$ can be found in Tables S3 and S4, respectively.

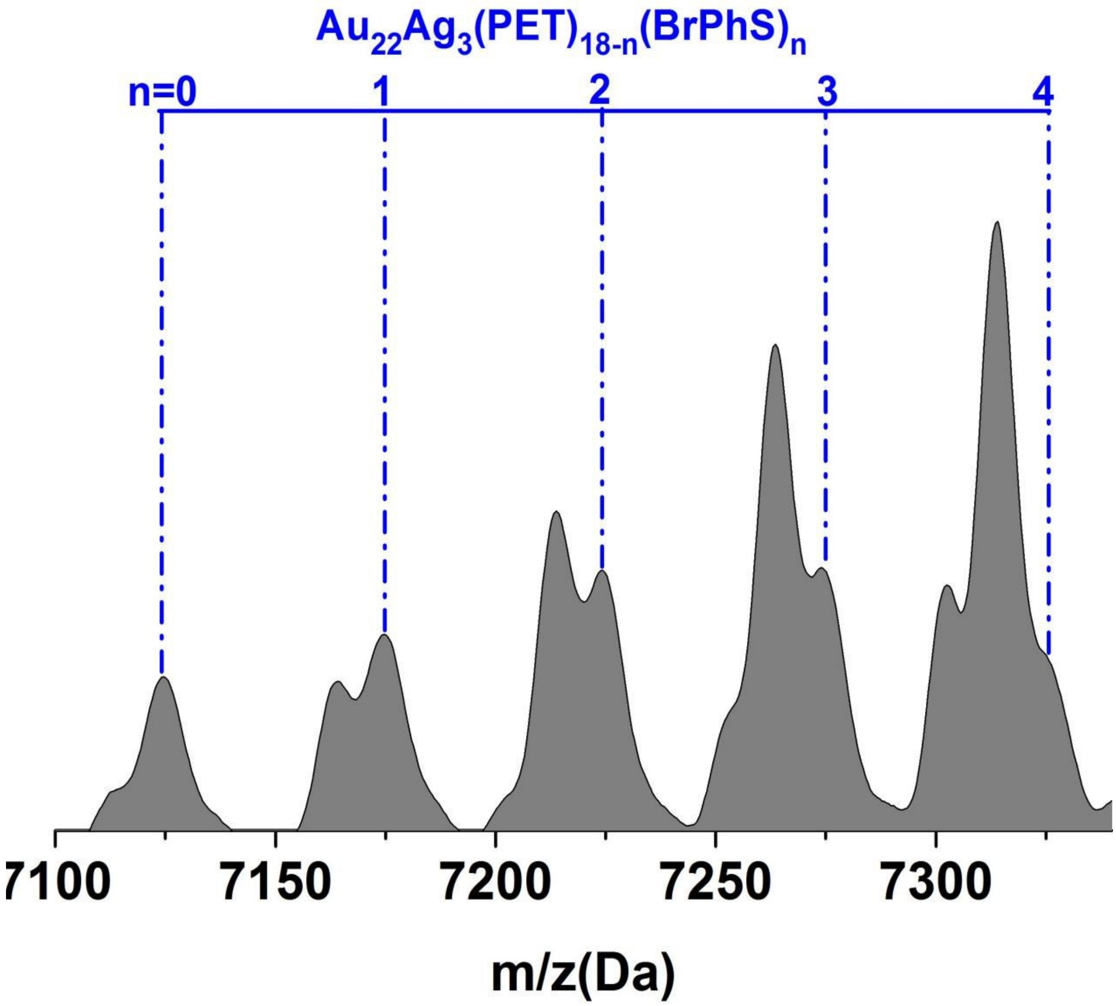

Fig. S11 MALDI-MS spectra of $Au_{22}Ag_3(PET)_{18-n}(SPhBr)_n$ corresponding to stage 7. The specific m/z and intensity of $Au_{22}Ag_3(PET)_{18-n}(SPhBr)_n$ can be found in Tables S3 and S4, respectively.

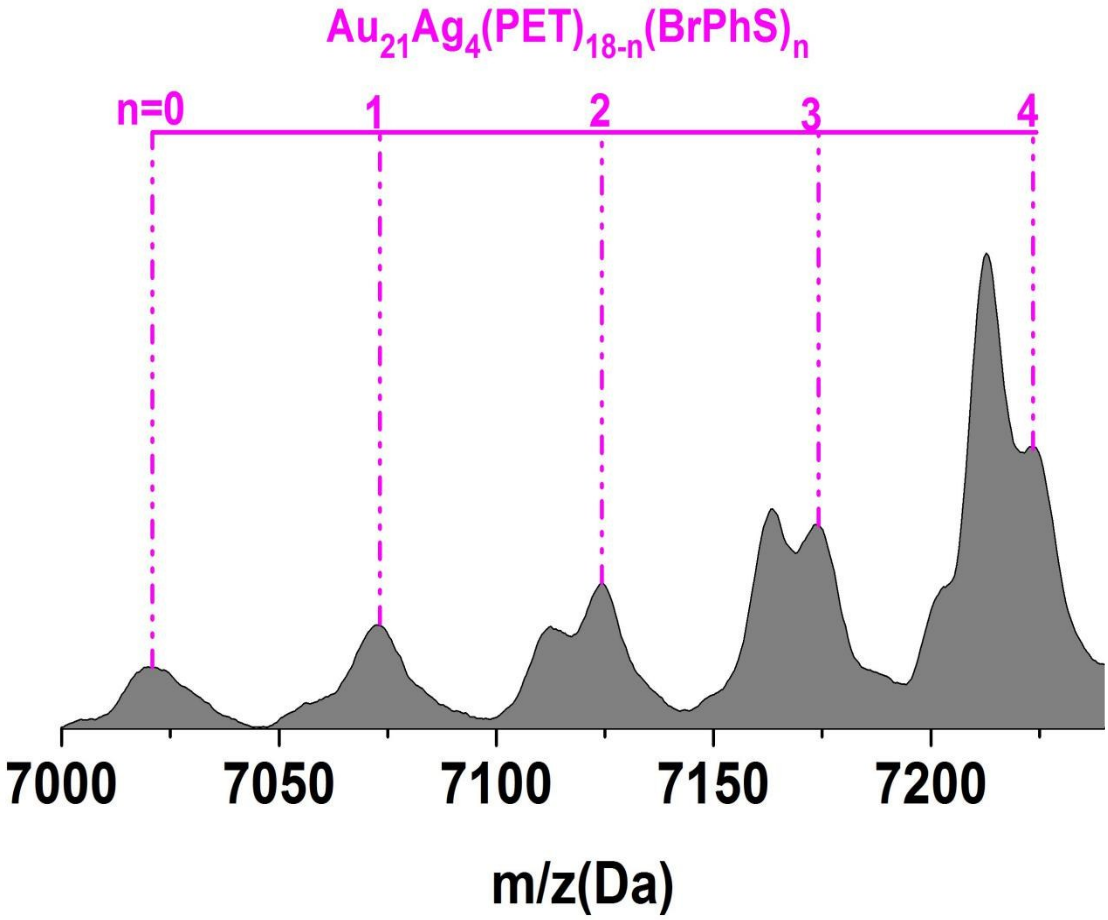

Fig. S12 MALDI-MS spectra of $Au_{21}Ag_4(PET)_{18-n}(SPhBr)_n$ corresponding to stage 7. The specific m/z and intensity of $Au_{21}Ag_4(PET)_{18-n}(SPhBr)_n$ can be found in Tables S3 and S4, respectively.

Table S1. The m/z values of different products which detected from the spectra of doping parent $Au_{25}(PET)_{18}$ with Ag-SC_2H_5.

m/z (Da)	nanoclusters
7392	$Au_{25}(PET)_{18}$
7316	$Au_{25}(PET)_{17}(EM)_1$
7240	$Au_{25}(PET)_{16}(EM)_2$
7303	$Au_{24}Ag_1(PET)_{18}$
7227	$Au_{24}Ag_1(PET)_{17}(EM)_1$
7151	$Au_{24}Ag_1(PET)_{16}(EM)_2$
7075	$Au_{24}Ag_1(PET)_{15}(EM)_3$
6999	$Au_{24}Ag_1(PET)_{14}(EM)_4$
7214	$Au_{23}Ag_2(PET)_{18}$
7138	$Au_{23}Ag_2(PET)_{17}(EM)_1$
7062	$Au_{23}Ag_2(PET)_{16}(EM)_2$
6986	$Au_{23}Ag_2(PET)_{15}(EM)_3$
6910	$Au_{23}Ag_2(PET)_{14}(EM)_4$
6834	$Au_{23}Ag_2(PET)_{13}(EM)_5$
7125	$Au_{22}Ag_3(PET)_{18}$
7049	$Au_{22}Ag_3(PET)_{17}(EM)_1$
6973	$Au_{22}Ag_3(PET)_{16}(EM)_2$
6897	$Au_{22}Ag_3(PET)_{15}(EM)_3$
6821	$Au_{22}Ag_3(PET)_{14}(EM)_4$
6754	$Au_{22}Ag_3(PET)_{13}(EM)_5$
7036	$Au_{21}Ag_4(PET)_{18}$
6960	$Au_{21}Ag_4(PET)_{17}(EM)_1$
6884	$Au_{21}Ag_4(PET)_{16}(EM)_2$
6808	$Au_{21}Ag_4(PET)_{15}(EM)_3$
6732	$Au_{21}Ag_4(PET)_{14}(EM)_4$

Table S2. The intensity of different products detected from the MALDI-MS spectra of doing the parent $Au_{25}(PET)_{18}$ with Ag-SC_2H_5 in different stages.

Intensity / nanocluster	stage						
	1	2	3	4	5	6	7
$Au_{25}(PET)_{18}$	7456	50973	10727	2853	210	0	0
$Au_{25}(PET)_{17}(EM)_1$		1621	3845	1930	265	0	0
$Au_{25}(PET)_{16}(EM)_2$		0	806	833	244	0	0
$Au_{24}Ag_1(PET)_{18}$		2929	3981	2968	654	83	0
$Au_{24}Ag_1(PET)_{17}(EM)_1$		278	1958	2614	1085	139	
$Au_{24}Ag_1(PET)_{16}(EM)_2$		319	612	1188	981	1237	
$Au_{24}Ag_1(PET)_{15}(EM)_3$		179	203	415	575	238	
$Au_{24}Ag_1(PET)_{14}(EM)_4$		0	103	151	275	0	0
$Au_{24}Ag_1(PET)_{13}(EM)_5$		0	0	0	99	0	0
$Au_{24}Ag_1(PET)_{12}(EM)_6$		0	0	0	0	0	0
$Au_{23}Ag_2(PET)_{18}$		0	748	1315	1071	210	22
$Au_{23}Ag_2(PET)_{17}(EM)_1$			435	1238	1967	531	68
$Au_{23}Ag_2(PET)_{16}(EM)_2$				756	1784	647	89
$Au_{23}Ag_2(PET)_{15}(EM)_3$				305	920	652	0
$Au_{23}Ag_2(PET)_{14}(EM)_4$				157	410	433	0
$Au_{23}Ag_2(PET)_{13}(EM)_5$				000	127	263	0
$Au_{22}Ag_3(PET)_{18}$				500	834	524	73
$Au_{22}Ag_3(PET)_{17}(EM)_1$				392	1598	1232	181
$Au_{22}Ag_3(PET)_{16}(EM)_2$				312	1399	1416	230
$Au_{22}Ag_3(PET)_{15}(EM)_3$					768	1199	164
$Au_{22}Ag_3(PET)_{14}(EM)_4$					330	709	69
$Au_{22}Ag_3(PET)_{13}(EM)_5$					105	320	25
$Au_{22}Ag_3(PET)_{12}(EM)_6$					32	190	12
$Au_{21}Ag_4(PET)_{18}$				243	379	539	81
$Au_{21}Ag_4(PET)_{17}(EM)_1$						1038	196
$Au_{21}Ag_4(PET)_{16}(EM)_2$						1140	219
$Au_{21}Ag_4(PET)_{15}(EM)_3$						921	158
$Au_{21}Ag_4(PET)_{14}(EM)_4$						524	0
$Au_{21}Ag_4(PET)_{13}(EM)_5$						161	0
$Au_{21}Ag_4(PET)_{12}(EM)_6$							0
$Au_{20}Ag_5(PET)_{18}$							29
$Au_{20}Ag_5(PET)_{17}(EM)_1$							7

Table S3. The m/z values of different products which detected from the spectra of doping parent $Au_{25}(PET)_{18}$ with Ag-SPhBr.

m/z (Da)	**nanocluster**
7392	$Au_{25}(PET)_{18}$
7443	$Au_{25}(PET)_{17}(SPhBr)_1$
7494	$Au_{25}(PET)_{16}(SPhBr)_2$
7303	$Au_{24}Ag_1(PET)_{18}$
7354	$Au_{24}Ag_1(PET)_{17}(SPhBr)_1$
7405	$Au_{24}Ag_1(PET)_{16}(SPhBr)_2$
7456	$Au_{24}Ag_1(PET)_{15}(SPhBr)_3$
7507	$Au_{24}Ag_1(PET)_{14}(SPhBr)_4$
7214	$Au_{23}Ag_2(PET)_{18}$
7265	$Au_{23}Ag_2(PET)_{17}(SPhBr)_1$
7316	$Au_{23}Ag_2(PET)_{16}(SPhBr)_2$
7367	$Au_{23}Ag_2(PET)_{15}(SPhBr)_3$
7418	$Au_{23}Ag_2(PET)_{14}(SPhBr)_4$
7469	$Au_{23}Ag_2(PET)_{13}(SPhBr)_5$
7125	$Au_{22}Ag_3(PET)_{18}$
7176	$Au_{22}Ag_3(PET)_{17}(SPhBr)_1$
7227	$Au_{22}Ag_3(PET)_{16}(SPhBr)_2$
7278	$Au_{22}Ag_3(PET)_{15}(SPhBr)_3$
7329	$Au_{22}Ag_3(PET)_{14}(SPhBr)_4$
7380	$Au_{22}Ag_3(PET)_{13}(SPhBr)_5$
7036	$Au_{21}Ag_4(PET)_{18}$
7087	$Au_{21}Ag_4(PET)_{17}(SPhBr)_1$
7138	$Au_{21}Ag_4(PET)_{16}(SPhBr)_2$
7189	$Au_{21}Ag_4(PET)_{15}(SPhBr)_3$
7240	$Au_{21}Ag_4(PET)_{14}(SPhBr)_4$

Table S4. The intensity of different products detected from the MALDI-MS spectra of doing the parent $Au_{25}(PET)_{18}$ with Ag-SPhBr in different stages.

Intensity / nanocluster	stage						
	1	2	3	4	5	6	7
$Au_{25}(PET)_{18}$	2005	3252	2853	9721	4655	2883	2615
$Au_{25}(PET)_{17}(SPhBr)_1$		395	1297	6521	4562	4308	4483
$Au_{25}(PET)_{16}(SPhBr)_2$		53	282	1893	1616	2763	3559
$Au_{24}Ag_1(PET)_{18}$		568	957	5634	3823	4308	6803
$Au_{24}Ag_1(PET)_{17}(SPhBr)_1$		168	863	5980	5300	7529	10539
$Au_{24}Ag_1(PET)_{16}(SPhBr)_2$			523	3501	3093	6756	11699
$Au_{24}Ag_1(PET)_{15}(SPhBr)_3$			233	1187	1251	2763	6587
$Au_{24}Ag_1(PET)_{14}(SPhBr)_4$				465	419	957	2379
$Au_{23}Ag_2(PET)_{18}$			85	1187	1251	22883	7511
$Au_{23}Ag_2(PET)_{17}(SPhBr)_1$			135	1532	1709	4689	12407
$Au_{23}Ag_2(PET)_{16}(SPhBr)_2$				1352	1803	5462	13567
$Au_{23}Ag_2(PET)_{15}(SPhBr)_3$				1350	1158	3536	11247
$Au_{23}Ag_2(PET)_{14}(SPhBr)_4$						1468	5191
$Au_{22}Ag_3(PET)_{18}$					419	1338	4719
$Au_{22}Ag_3(PET)_{17}(SPhBr)_1$					419	1730	5879
$Au_{22}Ag_3(PET)_{16}(SPhBr)_2$						1730	6351
$Au_{22}Ag_3(PET)_{15}(SPhBr)_3$						1980	6587
$Au_{22}Ag_3(PET)_{14}(SPhBr)_4$						1338	4955
$Au_{21}Ag_4(PET)_{18}$							2324
$Au_{21}Ag_4(PET)_{17}(SPhBr)_1$							3452
$Au_{21}Ag_4(PET)_{16}(SPhBr)_2$							4814
$Au_{21}Ag_4(PET)_{15}(SPhBr)_3$							4770
$Au_{21}Ag_4(PET)_{14}(SPhBr)_4$							0
$Au_{21}Ag_4(PET)_{13}(SPhBr)_5$							0
$Au_{21}Ag_4(PET)_{12}(SPhBr)_6$							0